electronics

MDPI

Article

AD8232 to Biopotentials Sensors: Open Source Project and Benchmark

José Jair Alves Mendes Junior [1,*], Daniel Prado Campos [2], Lorenzo Coelho de Andrade Villela De Biassio [1], Pedro Carlin Passos [1], Paulo Broniera Júnior [3], André Eugênio Lazzaretti [1] and Eddy Krueger [4]

1 Graduate Program in Electrical Engineering and Industrial Informatics (CPGEI), Federal University of Technology—Paraná (UTFPR), Sete de Setembro, 3165, Curitiba 80230-901, Brazil
2 Graduate Program in Biomedical Engineering (PPGEB), Federal University of Technology—Paraná (UTFPR), Marcílio Dias, 635, Apucarana 86812-460, Brazil
3 Senai Institute of Information and Communication Technology (ISTIC), Electronic System Laboratory—Embedded and Power Electronics, IoT and 4.0 Manufacturing, Rua Belém 844, Londrina 86026-040, Brazil
4 Anatomy Department, Neural and Rehabilitation Engineering Laboratory, State University of Londrina, Rodovia Celso Garcia Cid-Pr 445, Km 380, Londrina 86057-970, Brazil
* Correspondence: jjjunior@utfpr.edu.br

Abstract: Acquiring biopotentials with fidelity using low-cost circuits is a significant challenge in biomedical instrumentation. In this perspective, our goal is to investigate the characteristics of the widely applied AD8232®, an analog front-end for biopotential acquisition. We designed and evaluated circuits to acquire the most common biosignals: electrocardiogram (ECG), electromyogram (EMG), and electroencephalogram (EEG). Our findings show that the circuit is suitable for ECG and EMG instrumentation, although it has limitations for EEG signals, particularly concerning the gain. The entire project of the boards is also a contribution of this work as we intend to corroborate open-source do-it-yourself biomedical instrumentation.

Keywords: low-cost; electronic instrumentation; biomedical engineering; electromyography; electrocardiography; electroencephalography

check for updates

Citation: Mendes Junior, J.J.A.; Campos, D.P.; Biassio, L.C.d.A.V.D.; Passos, P.C.; Júnior, P.B.; Lazzaretti, A.E.; Krueger, E. AD8232 to Biopotentials Sensors: Open Source Project and Benchmark. *Electronics* **2023**, *12*, 833. https://doi.org/10.3390/electronics12040833

Academic Editor: Djuradj Budimir

Received: 2 January 2023
Revised: 31 January 2023
Accepted: 3 February 2023
Published: 7 February 2023

Copyright: © 2023 by the authors. Licensee MDPI, Basel, Switzerland. This article is an open access article distributed under the terms and conditions of the Creative Commons Attribution (CC BY) license (https://creativecommons.org/licenses/by/4.0/).

1. Introduction

The acquisition of biopotentials is one of the challenges in biomedical applications. The circuits have some desired characteristics, such as (i) having a high signal–noise ratio, (ii) high-gain amplification, (iii) easy construction, (iv) low-energy consumption, and (v) low cost of components [1,2]. The electronics development allowed the miniaturization of integrated circuits, where it did not need to design several circuits with operational amplifiers in a board: the biomedical front-ends could be developed in a single chip [1,3,4]. It supported the modularization of circuits, especially biomedical sensors, whereupon low-cost modules such as Bitalino® [5], Myoware® [6], OpenBCI platform® [7], among others (such as muscle sensors and electrocardiogram modules [8]). These devices have an easy connection with microcontrollers, which is one of the advantages of its use [9]. The applications with these modules involved the detection of biological parameters, such as QRS (Q, R, and S waves) complex [10], fatigue [11], and drowsiness [12], control prosthesis and robotics [13,14], and brain-machine interfaces [15–17].

One of the commercial solutions is the AD8232®. It is an integrated circuit for biopotential measurements, especially for electrocardiogram applications [18]. Furthermore, AD8232® integrated circuit has some advantages, such as its Low-Energy consumption (about 170 µA), rail-to-rail architecture, amplification, and filtering project in one single chip, and single supply [18,19]. Due to its features, a module for ECG acquisition was developed by SparkFun using the AD8232® [8]. It supports its use for a considerable number

of works and applications, such as the development of portable monitoring systems [20,21], detection of individuals [22], arrhythmias and abnormalities [23,24].

An alternative to the AD8232 is the chips from the from Texas Instrument's ADC129X® family, which are low-Noise, multichannel, 24-Bit Analog-to-Digital Converter (ADC) for Biopotential Measurements with Integrated ECG, EMG or EEG front-end [25]. This solution's advantages are the high-resolution ADC, programmable gain amplifiers, internal reference generator, onboard oscillator, a flexible input selected multiplexer, and SPI-compatible communication. On-chip ADC and digital interface could significantly simplify peripheral circuits. Nonetheless, setting the device for basic data capture requires a configuration routine on the microcontroller program to set up all the registers. Moreover, a set of external circuits must be included in the project to match design procedures, such as setting gains and power supply. Therefore, the final layout may have a more significant size concerning our object of study.

Unlike the front-end of other biopotentials, the AD8232® has a single channel and does not include an analog-to-digital converter (ADC). This may result in a less powerful instrument in terms of resolution and number of channels, but a more straightforward and compact solution if (i) a single channel is suitable for the project; or (ii) being compact is more important than having a high-resolution digital signal (when the microcontroller ADC suffices). AD8232 may be a better solution for wearable devices, and AD129x for powerful high-fidelity instruments.

Several works and circuits only use the AD8232® module for other biopotentials, such as Electromyography and Electroencephalography applications. However, each biopotential has intrinsic characteristics. ECG ranges from 0.5 mV to 4 mV and 0.01 Hz to 250 Hz of frequency; EMG from 0.1 mV to 5 V and frequencies until 10 kHz; and EEG from 5 µV to 300 µV and frequencies from 0 to 30 Hz [26]. In certain conditions, their characteristics suffer a change in their spectrum: ECG for monitoring rate can reach 40 Hz of frequency, and modern ECG machines can operate until 100 Hz [27], surface EMG (sEMG) could be a bandwidth of 20 Hz to 500 Hz [28], and each wave on EEG has its respective bandwidth (e.g., alpha waves range from 8 to 13 Hz) [29].

Some applications use the same module for ECG, EMG, and EEG acquisition [30–33], without changing the cutoff frequencies on the filter of gain adjustment for the parameters mentioned above. It is a crucial issue in biopotential circuit design. Moreover, even though these adaptations were performed (as presented in [34]), some tests were necessary to guarantee the gain and bandwidth for the required biopotential, assuring that the circuit matched for the purpose application. This is one of the problems of this type of application because, as the acquisition requirements are not met, the applications developed may suffer drops in their performance or be incorrectly met because the acquisition system is inadequate. Therefore, analyzing the electronic parameters of this type of system is necessary to guarantee that the circuits are suitable for acquiring biopotentials.

In this perspective, our goal is to present the electrical characteristics of AD8232® as an acquisition circuit for the most used biopotential signals: electrocardiogram, electromyogram, and electroencephalogram. We detail the project of the components and circuit board to be provided as well as the effects of electrical parameters, showing missing information about their use for both the ECG commercial module and their performance for the other biopotential circuits, being the original contribution of this work. Therefore, this work has two main contributions: (1) the evaluation of the AD8232 circuit as an analog front-end for biosignals acquisition beyond ECG; (2) The open source project of ECG, EMG, and EEG signal acquisition circuits using the AD8232.

This paper is organized as follows. Section 2 details the proposed circuit, evaluation procedures, and experimental methodology. Section 3 outlines the conducted experiments and their results, with the discussions and comparisons reported in Section 4. Section 5 shows the conclusions and future research directions.

2. Material and Methods

This section presents the features and description of the integrated circuit, the step-by-step, and the methodology employed to evaluate the circuits. This study was conducted with the approval of the Ethical Committee of the State University of Londrina (protocol number 3.004.069).

2.1. Features and Circuit Design Using AD8232®

Figure 1 presents the schematic of the projected circuit, which will be used to detail each part of the developed board. As a biopotential signal conditioning circuit, the AD8232® has an instrumentation amplifier with a fixed gain (100) and amplifiers that allow designing a high-pass and a low-pass filter. The high-pass is coupled with the instrumentation amplifier, and an operational amplifier is used to design the low-pass filter. Moreover, the circuit has a Right Leg Drive (RLD) and a buffer to set a DC level for output offset. A battery of 2 V from 3.5 V can supply the circuit. The IC did not need a symmetrical power source [18]. There are several possible filters and peripheral typologies, as detailed by [18]. In this work, we present the project and characteristics of a commonly used topology of the biopotentials circuit for AD8232®: instrumentation amplifier with second-order high and low-pass filters with offset on output.

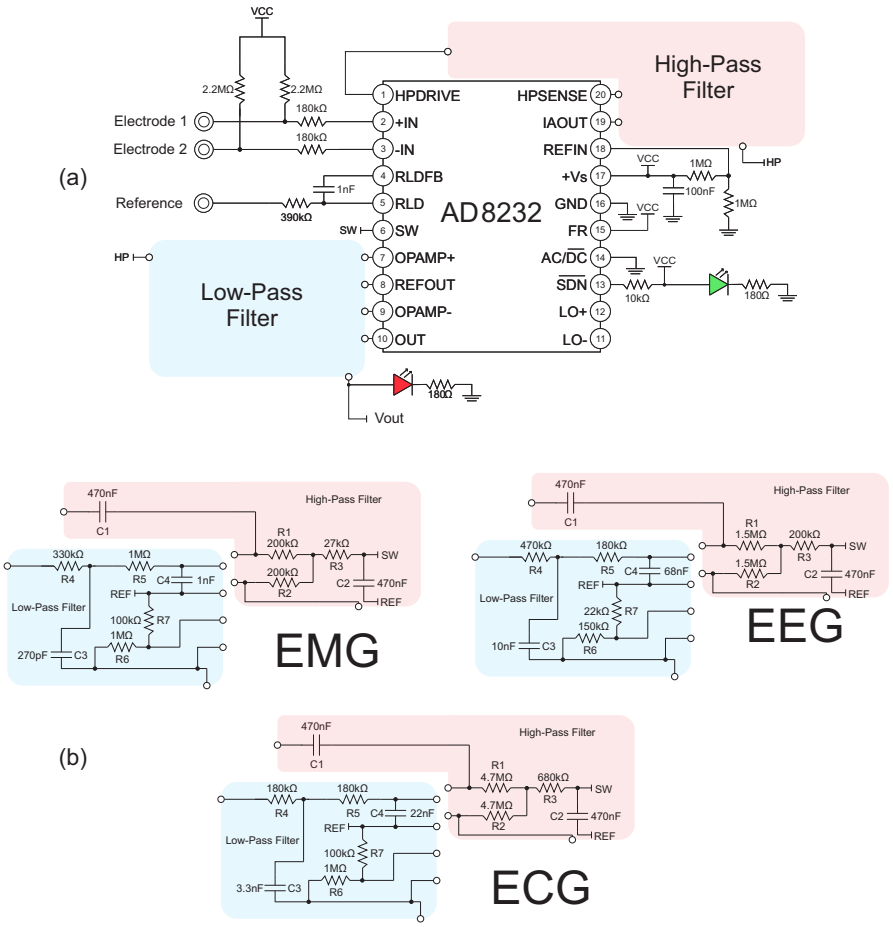


Figure 1. Schematic of the developed circuit. (**a**) A complete circuit schematic, with the components that are not changed during each biopotential design. The high-pass and low-pass filter placement are highlighted and detailed in (**b**) for the three chosen biopotentials.

The first stage of the circuit is the instrumentation amplifier. It has a fixed gain of 100× and a common-mode rejection rate (CMRR) informed by the manufacturer of 80 dB [18]. Their inputs (pins 2 and 3) have a resistor to limit the current when the input voltages

surpass the supply voltage and two pull-up resistors (2.2 MΩ) connected to the supply for leads-off detection.

Internally connected with the instrumentation amplifier, the high-pass filter is linked with pins 1, 19, and 20 with resistors and capacitors. The cutoff frequency for the high-pass filter (f_{cHP}) can be calculated by the following relation:

$$f_{cHP} = \frac{10}{2\pi\sqrt{R_1 R_2 C_1 C_2}}. \quad (1)$$

R_1, R_2, C_1 and C_2 are the resistors and capacitors, respectively, specified on the high-pass filter design of Figure 1b. This filter attenuates the low-frequency interference, mainly by motion artifacts and half-cell potential. Besides that, the AD8232 presents a second-order topology for the high-pass, which needs a compensation resistor to adjust this filter. Its relation is:

$$R_3 = 0.14 R_1. \quad (2)$$

The second-order low-pass filter can be projected by adding the operational amplifier in the circuit (pins 7, 8, and 10). Its topology can be seen in Figure 1b, and it is used to delimit the band of the desired biopotentials and attenuate the high frequencies. The cutoff frequency (f_{cLP}) can be calculated by:

$$f_{cLP} = \frac{1}{2\pi\sqrt{R_4 R_5 C_3 C_4}}. \quad (3)$$

R_4, R_5, C_3, and C_4 are the resistors and capacitor specified on low-pass filter of Figure 1b. As the filter is active, the gain of the circuit ($Gain_{LP}$) could be set by the resistor R_6 and R_7:

$$Gain_{LP} = 1 + \frac{R_6}{R_7}. \quad (4)$$

According to the manufacturer, the maximum gain that AD8232 could provide is 1100 (60.8 dB). Then, the maximum gain for the active filter that can be projected is 11.

The RLD circuit (pins 4 and 5 on Figure 1a) has a resistor of 390 kΩ to limit the current on the reference electrode. Pin 4 is the RLD feedback, which is connected to a capacitor of 1 nF to build an integrator to increase the CMRR of the obtained signal.

Pin 18 (REFIN) has the output voltage reference, which is half of the supply voltage. Two resistors of 1 MΩ define this reference. The circuit has a fast restore circuit, which is controlled by pin 15 (FR), and its terminal is pin 6 (SW). Pin 6 is connected to the output of the second high-pass filter. Pin 13 controls shutdown mode (which is always on high), and pins 11 and 12 are not connected because the leads-off detection was not implemented (pin 14 on low level). At last, two LEDs indicate that the circuit is supplied (green light) as well as the magnitude of the output signal (red light).

With the same circuit presented in Figure 1a, three biopotential circuits were projected, as illustrated in Figure 1b. For EMG, a gain of 60 dB and a frequency range from 20 Hz to 500 Hz were selected. For the EEG, the alpha wave rhythm was used to easily identify its occurrence on the signal (its presence when the subject closes his eyes [35]). Its bandwidth was projected from 8 Hz to 13 Hz, and due to its selectivity, a gain of about 55 dB was designed. At least, an ECG circuit was projected to present other possibilities without including a commercial module. A gain of about 60 dB was selected and the range of 0.7 Hz to 100 Hz was adopted, which makes it possible to verify the cardiac rate, similarly to [27]. One of the project criteria was the quality factor of the filter, which was chosen near 0.7 to provide a flat response (characteristic of Butterworth approximation, used in biopotential acquisition circuits [36]). The resistors' values are presented in Figure 1b for each configuration.

2.2. Experimental Methodology

Firstly, the electrical parameters were extracted from the commercial module AD8232—Single Lead Heart Rate Monitor AD8232® [8],—as this device has been used in several applications. Therefore, the electrical parameters of the proposed circuit were measured.

The Common Mode Rejection Rate (CMRR) of AD8232 was measured using the circuit presented in Figure 2 using the commercial module. This test was performed to determine this parameter from the electromagnetic noise from the main supply (60 Hz). Two wave generators were used: one autotransformer connected to the main supply and another wave generator with fixed amplitude and frequency (2 mV and 1 Hz). Peak-to-peak voltage from the autotransformer was changed to 1 from 200 Vpp (1 Vpp of step). The output of the AD8232 module was measured in the oscilloscope (Tektronix TDS 2002B) and the common and differential gain were measured, and the CMRR was calculated by:

$$CMRR = 20 \cdot log_{10}\left(\frac{|A_d|}{A_c}\right), \quad (5)$$

in which A_d is the differential gain and A_c is the common gain, both dimensionless.

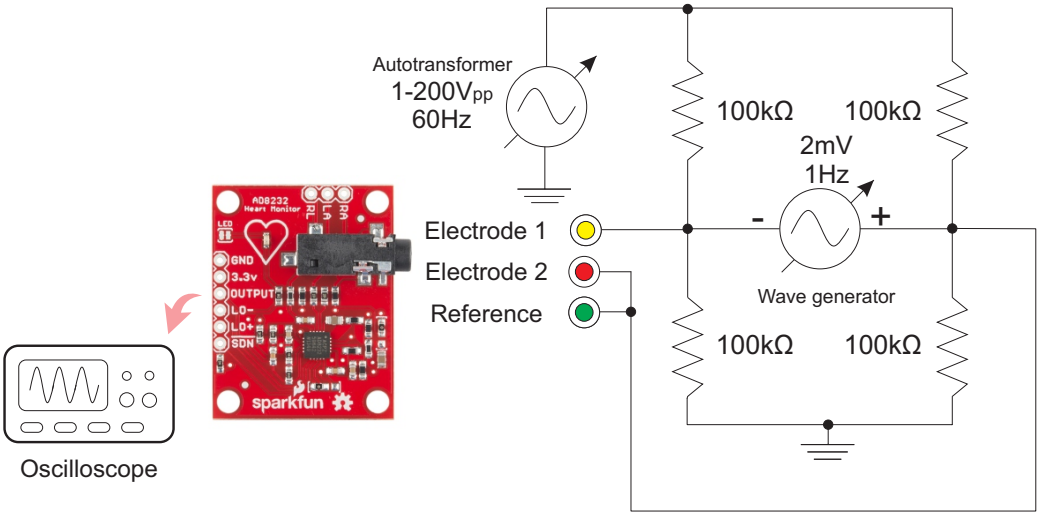


Figure 2. Setup to measure the CMRR of the AD8232 circuit. Two wave generators excite the input signal: an autotransformer and a wave (function) generator. The autotransformer excites with 60 Hz for several amplitudes, and the function generator excites the circuit with a 2 mV/1 Hz wave.

Concerning gain and bandwidth, the proposed circuit and commercial module were simulated to test the calculated values of the components. Tina-TI simulation tool software and AD8232 Filter Design were used to simulate the amplitude and calculate the circuit's bandwidth. On the board, the test of bandwidth frequency was performed using a wave generator to excite a known signal with varying frequencies, and an oscilloscope measured the output data from the board. The collected data were recorded and compared with the signals obtained through the simulation. For the commercial module, we evaluate the range of 0.02 Hz to 400 Hz; for EMG, from 0.5 Hz to 3,000 Hz; for EEG, from 0.03 Hz to 100 Hz; for ECG, from 0.05 Hz to 700 Hz.

Subsequently, the gain of the amplifier of the board was analyzed. The signals were generated using the same device with a fixed frequency and using a resistive voltage divider (with a resistor with 1% of precision) to reduce the signal amplitude. The frequencies were based on the middle of bandwidth for each circuit: ECG was defined as 20 Hz, 200 Hz for ECG, and 6 Hz for EEG. Output was acquired via an oscilloscope.

Thus, the biopotential signals were acquired using the three circuits. The circuit was supplied by batteries to isolate the volunteer from the main supply, and the signals were sent to a microcontroller ESP32 Devkit, as presented in Figure 3. This microcontroller

acquired the data from the serial with a fixed sampling frequency (1 kHz for EMG and ECG and 1 Hz for EEG), which can acquire the selected biopotential by the Nyquist criterion. Moreover, the microcontroller has a 12-bit analog-digital converter resolution, which is suitable for biomedical signals. The data were acquired from a computer without connection with the main supply. The EMG signal was acquired from the biceps brachii muscle using differential electrodes connected to the inputs. The reference electrode was placed on the olecranon. The ECG circuit was tested by placing the electrodes in a Lead I configuration. Three disposable Ag/AgCl gel electrodes were used in both ECG and EMG.

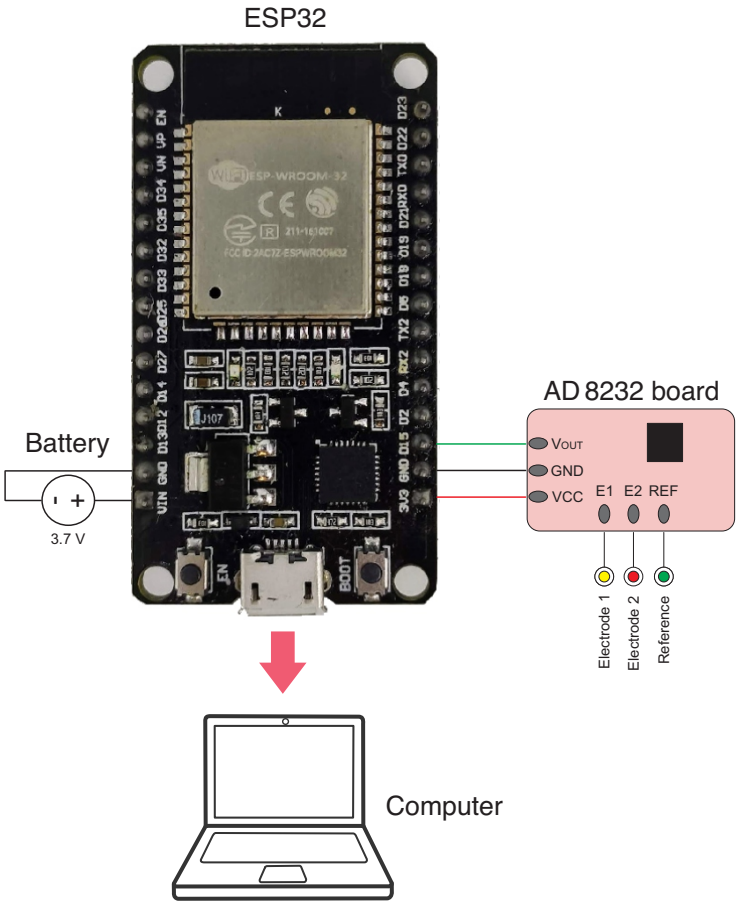


Figure 3. Schematic of connection of AD8232 board and the ESP32 Devkit module.

The electrode cap from OpenBCI® was employed for EEG. The inputs were connected following the 10–20 system employed for OpenBCI®: Cz and O1 (Occipital left side) for the differential electrodes, and T4 was connected to the reference. A conductive gel was inserted on the electrodes to increase the skin-electrode interface and to facilitate the acquisition. A passive 60 Hz-notch filter was implemented at the output of the EEG circuit to increase the signal–noise ratio. The volunteer was oriented to close his eyes for three seconds to acquire an alpha wave.

At last, the energy consumption for the circuit was measured. The ammeter was employed to measure the current consumed by the board.

3. Results

The three circuits projected for the ECG, EMG, and EEG tests (seen in Figure 1) were soldered to the universal PCB developed for AD8232® based circuits, presented in Figure 4. This version of the universal board has 36 mm × 20 mm dimensions and ensures a tiny and reliable platform to test different high and low pass filter configurations.

The board uses male header connectors on both sides. On the left, it has all the differential electrode inputs (right arm—RA, left arm—LA, and right leg—RL); on the right, it has the ground and 3.3 V inputs and the signal wave output for data collection.

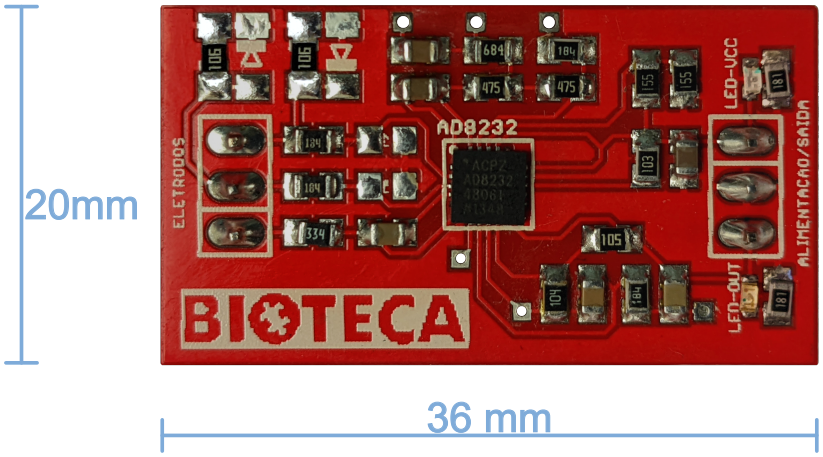


Figure 4. Universal PCB developed for AD8232-based circuits, with its dimensions.

Starting with the electrical parameters from the commercial module, Figure 5a presents the CMRR obtained from the AD8232® circuit. The datasheet informs that AD8232® has a CMRR of about 80 dB for 60 Hz frequency. However, one can note that this value starts from 60 dB in low peak-to-peak voltages and increases, stabilizing values close to 110 dB. It is important to note that for the main supply amplitude (180 Vpp, which represents 127 Vrms), the obtained CMRR was 113 dB, higher than provided for the manufacturer, which is a great advantage of this circuit. The attenuation for the interference of the main supply can reach about 450,000 times. Increasing the voltage interference (to the limits of the autotransformer), one can note that it did not change the values of CMRR, standing above 110 dB.

Regarding the frequency bandwidth, the commercial module has a projected range of 0.7 Hz to 40 Hz. Its maximum gain is 60.9 dB (about 1110 times). Figure 5b presents that its frequency range has minor differences: 0.74 Hz to 45 Hz, which is acceptable due to the precision of the components. The same tendency was observed in simulation values. Concerning the gain, there is a difference of about 1 dB between real and simulated (projected). Using D'Agostino-Pearson test [37], one can note that the gain distribution was not normally distributed (with an interval of confidence of 0.001). The maximum real gain obtained with the commercial module is near 989 V/V (59.9 dB). As heart rate monitor (ECG), as this circuit is commonly used, it does not represent a significant problem because the algorithms for these applications did not use the wave amplitude value to calculate this parameter. Nonetheless, it reinforces that this module could not be suitable for other biopotential acquisition/parameters without changing the electric components.

Figure 6 presents the obtained bandwidth and amplitude from the project circuit for (a) EMG, (b) EEG, and (c) ECG biosignals. In general, one can note that the bandwidths have similar behavior, except for the low frequencies on the high-pass filter, which presented visible differences. This variance is more prominent on the ECG bandwidth (about 10 dB for frequencies below 0.4 Hz). On the other hand, except for the ECG, the amplitudes between simulated and real values have a difference of about 2 dB, whose real values are higher than simulated.

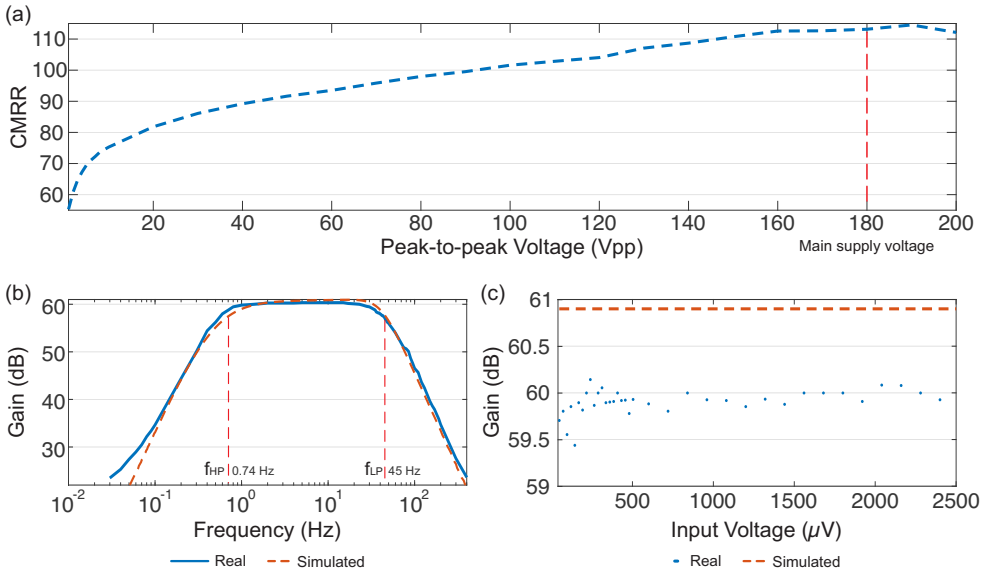


Figure 5. Parameters acquired from the commercial module AD8232: (**a**) CMRR in function of input voltage, (**b**) magnitude from Bode diagram, highlighting the low-pass and high-pass cutoff frequencies, and (**c**) the total gain of the circuit using a 20 Hz sinusoidal wave for several input amplitudes. Both simulated and real values are presented. In (**a**,**b**), f_{HP} and f_{LP} are the high and low cutoff frequencies, respectively.

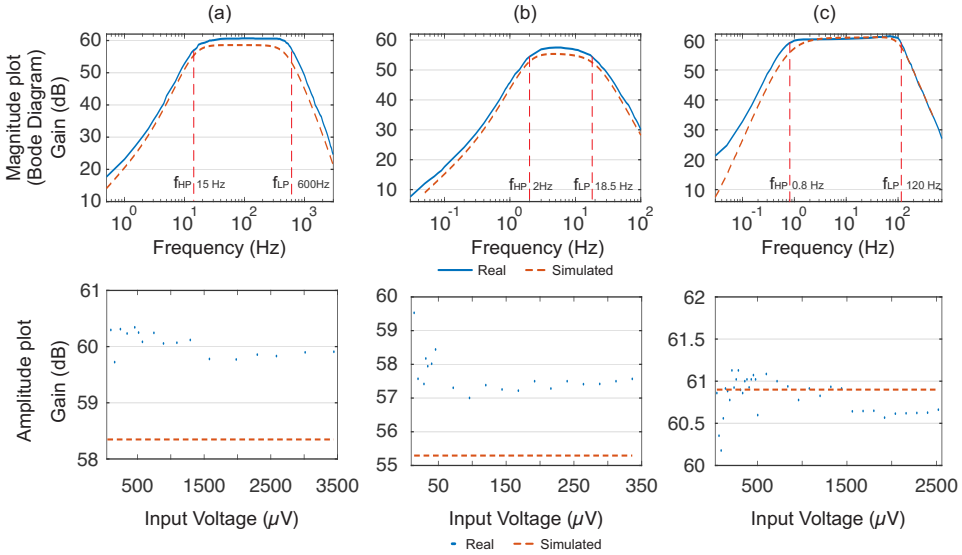


Figure 6. Magnitude plot from the Bode Diagram and obtained gains from the designed circuits for (**a**) EMG, (**b**) EEG, and (**c**) ECG biosignals. Both real and simulated values are presented. Filters' low-pass and high-pass cutoff frequencies are highlighted. In (**a**,**b**), f_{HP} and f_{LP} are the high and low cutoff frequencies, respectively.

The obtained ranges of frequencies from each biosignal were:

- EMG: 15 Hz to 600 Hz;
- EEG: 2 Hz to 18.5 Hz;
- ECG: 0.8 Hz to 120 Hz.

As the filters have second order, plane response, and the precision of electronic components, the frequency range is slightly more extensive. Among the cutoff frequencies, the most distant frequency was the low-pass frequency of the EMG circuit. Nevertheless, it did not represent a significant difference for the EMG bandwidth, knowing that signals with higher energy are presented up to frequencies of 150 Hz [38,39].

Concerning the amplitude plot, the EMG circuit presented an average real gain of 60.1 dB; EEG, 57.6 dB; and ECG, 60.8 dB. It was evaluated to check if the distribution of the gain was normal (using the D'Agostino-Person test) [37], and only the ECG circuit presented a normal distribution ($p < 0.005$).

Regarding the performance of the circuits, one can note that the AD8232 presents results from the ECG that are more approximate with these biosignal requirements. Comparing our design with the commercial design, one can note that the circuit allowed gains closer to what was projected than the commercial design, besides a normal distribution. It is a characteristic that can encourage hardware developers to use the AD8232, showing that it is possible to improve the circuit characteristics without using the commercial module.

The designed circuits were able to acquire biosignals (ECG, EMG, and EEG), although it was built especially for ECG (it is labeled as a "Heart Rate Monitor Front-End"). The system is suitable for EMG and ECG. However, there are some limitations regarding EEG signal acquisition. For example, identifying the alpha-wave pattern in EEG, as highlighted in Figure 7, is not a trivial task as for other biosignals. The EEG signal demands an instrumentation requirement that extrapolates the features of the AD8232 chip. For example, EEG acquisition circuits usually feature a gain higher than 1000 [40,41]. As the observed peak-to-peak amplitude of the EEG signal is around 300 µV, the reached gain may not optimize the AD range.

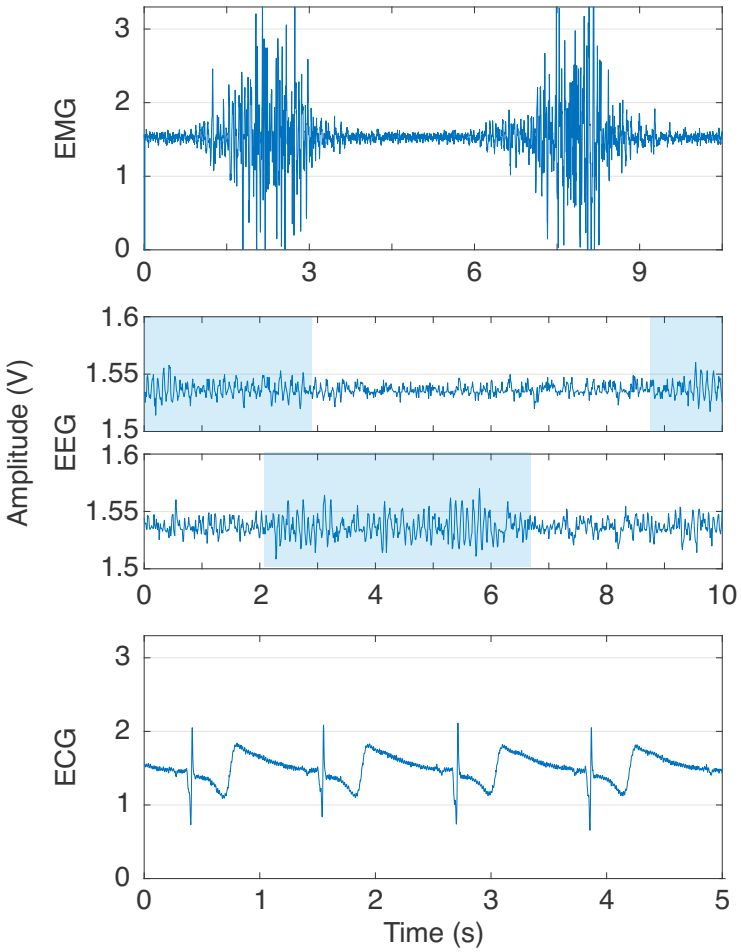


Figure 7. Signals acquired from each biopotential circuit: EMG from biceps brachii muscle, alpha-wave for EEG, and ECG acquired from Lead I configuration. In EEG, the alpha wave is highlighted when the volunteer closes his eyes, acquired from the volunteer using OpenBCI® electrode cap. Differential electrodes were used placed on O1 and Cz, while T4 was connected on reference, following the 10–20 System.

Although the AD8232 circuit can amplify close to 1100 times the input, the EEG circuit achieved around 750. As pointed out by the manufacturer, the filter roll-off prevents the maximum gain from reaching this value [18].

The 57 dB amplification requires a high resolution of the analog-to-digital converter of the microcontroller circuit responsible for acquiring the signals. Another point to mention is that the bandwidth of the used EEG circuit was straighter than the EMG and ECG. This could be one of the factors that affected the maximum gain obtained to guarantee the plan response designed for the filters. Increasing the gain changes the filter response, affecting the designed parameters. Therefore, the AD8232 could not be suitable for this biopotential acquisition.

4. Discussion

Remarkably, the AD8232® is vastly applied in ECG applications, mainly for portable healthcare systems and Internet of Things (IoT) applications. Its instrumented version is abundantly available in the market as an ECG module: a low-cost, low-consumption, small-size, ready-to-use, modular acquisition board [42–44]. Among other analog front-end chips for ECG signal acquisition, e.g., HM301D and ADS1191, it provides high enough gain to get good resolution and the best output impedance [45]. A few works focused on comparing and evaluating rather than applying the AD8232®. Usually, the evaluations are focused on an ECG or EMG device based on AD8232.

For example, in [19], the authors compared several EMG acquisition systems, including one based on the AD8232 chip. The acquired signal from each device was compared by visual inspection as the focus of the work was the potential for use in bionic hand prosthesis control systems.

A recurrent device based on the AD8232 chip is the Bitalino®. It is a ready-to-use modular platform developed by PLUX for biosignal acquisition. It has been used in wearables for healthcare for its simplicity in its design that facilitates the translation into industrial applications [46]. Its EMG and ECG modules are based on the AD8232 circuit [47,48]. The transient analysis resulted in 2.337 s time delay for the ECG circuit and a 0.146 s time delay for EEG due to the time constant of the integrator network at the first stage of the biosignal amplifier in both circuits [5]. In a comparison between Bitalino® and BioPac, which is standard equipment, a high correlation between the two was observed [49]. Nevertheless, an evaluation of gain and frequency bands was not the subject of this evaluation. Also, Bitalino's EEG circuits do not employ an AD8232 chip; therefore, it is not evaluated for this task in the papers mentioned above.

In [50], an ECG acquisition circuit was developed and compared to a system based on the AD8232® as ground truth. The chosen configuration was the "Cardiac Monitor Configuration", which has a 0.5 Hz two-pole high-pass filter followed by a two-pole, 40 Hz, low-pass filter and a total system gain of 1100 [18]. Electrical parameters were measured just from the developed circuit, and the acquired time-series waveforms from both were confronted. The measured frequency response from the developed device was compared to the curve provided in the chip's datasheet.

Although the device presented a suitable performance for biosignal acquisition, there is a drawback in the application of EEG. This may be why manufacturers, such as Plux Biosignals (Bitalino), are not using it for this purpose. On the other hand, even with the chip being designed for ECG, its performance for myoelectric signal acquisition meets expectations regarding gain, frequency response, and CMRR.

Comparison with Related Works

As previously mentioned, only some works in the literature develop their circuits using IC AD8232 without the developed module for ECG acquisition. For example, ref. [30] used the ECG commercial module and a 60 Hz notch filter to acquire EEG signals. Thus, the frequency band of the EEG (that can reach 100 Hz) was limited to the frequency band

of the ECG module, which was shown to be close to 45 Hz. Some frequencies could not be on the interesting band used in this work to detect alpha waves.

The same case occurs for the EMG signal, with its use only in the commercial module without modification [31,32]. On the other hand, the authors in [34] developed their circuit for acquiring EMG signals using the AD8232 circuit to identify drowsiness by steering wheel grip. The circuit was designed for a frequency band of 20 to 150 Hz, with a maximum gain of 780 (57.8 dB) [34]. The authors did not present the design parameters and corresponding analyses to verify whether the gain and frequency range matched the design criteria.

As the ECG signal acquisition module is commercially available, works that intend to acquire ECG signals with AD8232 use the commercial module. Some authors, such as [20,51] developed their own ECG circuit, but with the same values of resistors and capacitors as the commercial module. In particular, ref. [51] compared noise levels between an AD8232 circuit on a breadboard and a printed circuit board. The authors presented that the printed circuit board decreased about 3.5 times the amount of noise level than the circuit on a breadboard.

Concerning assistive technology implementations, currently, the use of non-invasive sensors that register the nervous system to assistive technology search are compact and modular to be wearable. An example is the work presented in [52], where the authors proposed a hardware that uses EMG and inertial sensors to estimate the motor intention to trigger functional electrical stimulation (FES) in lower limb muscles. In this sense, even just with one channel, the present paper shows that the EMG sensor dimensions (20 mm $\times$ 36 mm) are related to [52] (35 mm $\times$ 45 mm, 2 channels), and are viable to wearable implementations. Low-cost assistive devices are important mainly for poor countries, as in [53], that developed a 3D printed arm exoskeleton, Arduino® board programmed and smartphone-controlled (easier access than personal computer in poor countries). However, as a limitation, the arm exoskeleton is just controlled by smartphone, which jeopardizes the user experience. Thus, the user must use one hand (healthy and holding the smartphone) to control the other arm (affected limb), where the implementation of our sensor in proximal muscles (such as the shoulder area) can trigger the exoskeleton and allow the smartphone use just to perform the parameters selection.

As limitations, this work presents the application for the three main biopotential acquisition signals used in the literature for the AD8232 circuit, focusing on one-channel application. The present project should be updated, in order to improve the use to assistive technology use, such as size shrinkage and increasing channel numbers. Beyond EMG, ECG and EMG, our circuit can incorporate other human–machine sensors, such as force-myography [54] and/or mechanomyography [55].

5. Conclusions

In this work, we benchmarked the AD8232 chip in acquiring the three most common biosignals: ECG, EMG, and EEG. Our findings show that the circuit is suitable for ECG and EMG instrumentation, presenting feasible gain and frequency response. One of the project drawbacks is the gain limitation, which may not be suitable for EEG signal acquisition.

The full project of the filters and circuit topology is also a contribution as we intend to collaborate with open-source and do-it-yourself biomedical instrumentation projects. Therefore, with this work, we intend to test the chip for application beyond the ECG and provide a ready-to-use biosignal instrumentation circuit. The main challenge of the project was to design compact, accessible, open-source, low-cost, and do-it-yourself biopotential circuits for wearable assistive and medical devices. The project is a first step into a culture of making assistive technology, such as robotic orthoses and prostheses, accessible and reproducible for scientists and enthusiasts.

Future works may benchmark other commercially available biopotential front-ends. The main goal is to enable the reproducibility of low-cost, high-quality circuits for rehabilitation and assistive devices. This way, looking for alternatives to facilitate in-loco production of biomedical instrumentation should corroborate the dissemination of the technology. Fur-

thermore, improving biopotential acquisition circuits that enable miniaturization may ease the production of embedded systems such as robotic mioelectric orthosis and prosthesis, online ECG monitoring, and brain-machine interfaces.

Author Contributions: Conceptualization, J.J.A.M.J., D.P.C., A.E.L., P.B.J. and E.K.; Methodology, J.J.A.M.J., P.B.J. and L.C.d.A.V.D.B.; Software, J.J.A.M.J., L.C.d.A.V.D.B.; Validation, J.J.A.M.J., L.C.d.A.V.D.B. and P.C.P.; Formal Analysis, J.J.A.M.J., D.P.C.; Resources, J.J.A.M.J., D.P.C. and E.K.; Data Curation, L.C.d.A.V.D.B., P.C.P.; Investigation, J.J.A.M.J., L.C.d.A.V.D.B. and P.C.P.; Writing—Original Draft Preparation, J.J.A.M.J., D.P.C., L.C.d.A.V.D.B. and P.C.P.; Writing—Review & Editing, D.P.C., P.B.J., A.E.L. and E.K.; Visualization, J.J.A.M.J., D.P.C., P.B.J. and E.K.; Supervision, A.E.L. and E.K.; Project Administration, A.E.L. and E.K.; Funding Acquisition, J.J.A.M.J., D.P.C. and E.K. All authors have read and agreed to the published version of the manuscript.

Funding: This study was financed in part by the Federal University of Technology—Paraná.

Data Availability Statement: The project is presented entirely for reproduction in the following link github.com/LENeR-UEL/AD8232_aquisition_circuit.

Conflicts of Interest: The authors declare no conflict of interest.

References

1. Guerrero, F.N.; Spinelli, E.M. Biopotential Acquisition Systems. In *Medicine-Based Informatics and Engineering*; Simini, F., Bertemes-Filho, P., Eds.; Springer International Publishing: Cham, Switzerland, 2022; pp. 51–79. [CrossRef]
2. Nagel, J.H. Biopotential Amplifiers. In *Biomedical Engineering Handbook*; CRC Press: Boca Raton, FL, USA, 2000; Volume 1, pp. 1364–1377.
3. Heywood, S.; Pua, Y.H.; McClelland, J.; Geigle, P.; Rahmann, A.; Bower, K.; Clark, R. Low-cost electromyography—Validation against a commercial system using both manual and automated activation timing thresholds. *J. Electromyogr. Kinesiol.* **2018**, *42*, 74–80. [CrossRef] [PubMed]
4. Palumbo, A.; Vizza, P.; Calabrese, B.; Ielpo, N. Biopotential Signal Monitoring Systems in Rehabilitation: A Review. *Sensors* **2021**, *21*, 7172. [CrossRef] [PubMed]
5. Plácido da Silva, H.; Guerreiro, J.; Lourenco, A.; Fred, A.; Martins, R. BITalino: A Novel Hardware Framework for Physiological Computing. In Proceedings of the International Conference on Physiological Computing Systems, Lisbon, Portugal, 7–9 January 2014.
6. Advancer Technologies. 3-Lead Muscle Electromyography Sensor for Microcontroller Applications. Technical Report, Advancer Technologies 2015. Available online: https://cdn.sparkfun.com/assets/learn_tutorials/4/9/1/datasheet.pdf (accessed on 3 August 2022).
7. OpenBCI. OpenBCI, 2022. Available online: https://openbci.com/ (accessed on 4 August 2022).
8. Sparkfun. SparkFun Single Lead Heart Rate Monitor—AD8232, 2022. Available online: https://www.sparkfun.com/products/12650 (accessed on 4 August 2022).
9. Toledo Peral, C.L.; Vega Martínez, G.; Peralta Hernández, R.; Guadarrama Becerril, J.H.; Gilberto Franco Sánchez, J.; Gutiérrez Martínez, J.; Alvarado Serrano, C.; Vera Hernández, A.; Leija Salas, L. Experience of Use of the BiTalino Kit for Biomedical Signals Recording during Ergometric Test. In Proceedings of the 2020 17th International Conference on Electrical Engineering, Computing Science and Automatic Control (CCE), Phuket, Thailand, 24–27 June 2020l; pp. 1–6. [CrossRef]
10. Rodríguez-Jorge, R.; De León-Damas, I.; Bila, J.; Škvor, J. Internet of things-assisted architecture for QRS complex detection in real time. *Internet Things* **2021**, *14*, 100395. [CrossRef]
11. Yuliza, M.; Angraini, T.; Susanti, R.; Effendi; Isma, T.W. Ad8232 Sensor Implementation To Detect Fatigue. *IOP Conf. Ser.* **2020**, *846*, 12040. [CrossRef]
12. Hayawi, A.A.; Waleed, J. Driver's Drowsiness Monitoring and Alarming Auto-System Based on EOG Signals. In Proceedings of the 2019 2nd International Conference on Engineering Technology and its Applications (IICETA), Barcelona, Spain, 18–20 December 2019; pp. 214–218. [CrossRef]
13. Satya Sree, K.P.N.V.; Bikku, T.; Mounika, S.; Ravinder, N.; Kumar, M.L.; Prasad, C. EMG Controlled Bionic Robotic Arm using Artificial Intelligence and Machine Learning. In Proceedings of the 2021 Fifth International Conference on I-SMAC (IoT in Social, Mobile, Analytics and Cloud) (I-SMAC), Palladam, India, 11–13 November 2021; pp. 548–554. [CrossRef]
14. Omama, Y.; Haddad, C.; Machaalany, M.; Hamoudi, A.; Hajj-Hassan, M.; Ali, M.A.; Hamawy, L. Surface EMG Classification of Basic Hand Movement. In Proceedings of the 2019 Fifth International Conference on Advances in Biomedical Engineering (ICABME), Tripoli, Lebanon, 17–19 October 2019; pp. 1–4. [CrossRef]
15. Cardoso, V.F.; Delisle-Rodriguez, D.; Romero-Laiseca, M.A.; Loterio, F.A.; Gurve, D.; Floriano, A.; Valadão, C.; Silva, L.; Krishnan, S.; Frizera-Neto, A.; et al. Effect of a Brain–Computer Interface Based on Pedaling Motor Imagery on Cortical Excitability and Connectivity. *Sensors* **2021**, *21*, 2020. [CrossRef]

16. Autthasan, P.; Du, X.; Arnin, J.; Lamyai, S.; Perera, M.; Itthipuripat, S.; Yagi, T.; Manoonpong, P.; Wilaiprasitporn, T. A Single-Channel Consumer-Grade EEG Device for Brain–Computer Interface: Enhancing Detection of SSVEP and Its Amplitude Modulation. *IEEE Sens. J.* **2020**, *20*, 3366–3378. [CrossRef]
17. Abougarair, A.J.; Gnan, H.M.; Oun, A.; Elwarshfani, S.O. Implementation of a Brain-Computer Interface for Robotic Arm Control. In Proceedings of the 2021 IEEE 1st International Maghreb Meeting of the Conference on Sciences and Techniques of Automatic Control and Computer Engineering MI-STA, Tripoli, Libya, 25–27 May 2021; pp. 58–63. [CrossRef]
18. Analog Devices. AD8232: Single-Lead, Heart Rate Monitor Front End. Analog Devices, 2020. Available online: https://www.analog.com/media/en/technical-documentation/data-sheets/ad8232.pdf (accessed on 2 February 2022).
19. Eliseichev, E.A.; Mikhailov, V.V.; Borovitskiy, I.V.; Zhilin, R.M.; Senatorova, E.O. A Review of Devices for Detection of Muscle Activity by Surface Electromyography. *Biomed. Eng.* **2022**, *56*, 69–74. [CrossRef]
20. Bravo-Zanoguera, M.; Cuevas-González, D.; García-Vázquez, J.P.; Avitia, R.L.; Reyna, M.A. Portable ECG System Design Using the AD8232 Microchip and Open-Source Platform. *Proceedings* **2019**, *42*, 49. [CrossRef]
21. Prasad, A.S.; Kavanashree, N. ECG Monitoring System Using AD8232 Sensor. In Proceedings of the 2019 International Conference on Communication and Electronics Systems (ICCES), Coimbatore, India, 17–19 July 2019; pp. 976–980. [CrossRef]
22. Camacho-Perea, A.; Maya-Martinez, S.U.; Tovar-Corona, B.; De la Rosa-Montero, E.D. Electrocardiographic signal as a biometrie feature. In Proceedings of the 2017 14th International Conference on Electrical Engineering, Computing Science and Automatic Control (CCE), Mexico City, Mexico, 20–22 October 2017; pp. 1–5. [CrossRef]
23. Villegas, A.; McEneaney, D.; Escalona, O. Arm-ECG Wireless Sensor System for Wearable Long-Term Surveillance of Heart Arrhythmias. *Electronics* **2019**, *8*, 1300. [CrossRef]
24. Kanani, P.; Padole, M.C. Recognizing Real Time ECG Anomalies Using Arduino, AD8232 and Java. In *Advances in Computing and Data Sciences*; Springer: Singapore, 2018; pp. 54–64.
25. Instruments, T. ADS1299-x Low-Noise, 4-, 6-, 8-Channel, 24-Bit, Analog-to-Digital Converter for EEG and Biopotential Measurements, Texas Instruments, 2015. Available online: https://www.ti.com/lit/ds/symlink/ads1299.pdf (accessed on 20 January 2023).
26. Webster, J.G. *Medical Instrumentation: Application and Design*; John Wiley & Sons: Hoboken, NJ, USA, 2009.
27. Tereshchenko, L.G.; Josephson, M.E. Frequency Content and Characteristics of Ventricular Conduction. *J. Electrocardiol.* **2015**, *48*, 933–937. [CrossRef]
28. Luca, C.J.D. The Use of Surface Electromyography in Biomechanics. *J. Appl. Biomech.* **1997**, *13*, 135–163. [CrossRef]
29. Bateson, A.D.; Asghar, A.U.R. Development and Evaluation of a Smartphone-Based Electroencephalography (EEG) System. *IEEE Access* **2021**, *9*, 75650–75667. [CrossRef]
30. Neves, F.; Kanoh, S.; Maia, J. Development and evaluation of a low-cost electroenphalography measuring device. In Proceedings of the V Brazilian Congress of Electromyography and Kinesiology, Armação de Buzios, Brazil, 21–25 October 2018; p. 4. [CrossRef]
31. Samson, V.R.R.; Bharath Sai, U.; Pradeep Kumar, S.; Praveen Kitti, B.; Suresh Babu, D.; Madhuri, G.M.G.; Malleswararao, P.L.S.D.; Kedar Eswar, K. Human Hand Controlled by Other Human Brain. In *Recent Findings in Intelligent Computing Techniques*; Sa, P.K., Bakshi, S., Hatzilygeroudis, I.K., Sahoo, M.N., Eds.; Springer: Singapore, 2018; pp. 451–458. [CrossRef]
32. Hafid, A.; Medjek, M.; Bediaf, R.; Difallah, S. Affordable Custom made Physiological Measurement Instrumentation Based on Raspberry PI. In Proceedings of the 2022 7th International Conference on Image and Signal Processing and Their Applications (ISPA), Shenzhen, China, 27–29 May 2022; pp. 1–5. [CrossRef]
33. Seçkin, A. Labeling System with EEG, EMG, and IMU for Visual Training of Autonomous Vehicles. *J. Inf. Technol.* **2019**, *12*, 299–305. [CrossRef]
34. Satti, A.T.; Kim, J.; Yi, E.; Cho, H.y.; Cho, S. Microneedle Array Electrode-Based Wearable EMG System for Detection of Driver Drowsiness through Steering Wheel Grip. *Sensors* **2021**, *21*, 5091. [CrossRef]
35. Rao, R.P.N. *Brain-Computer Interfacing: An Introduction*; Cambridge University Press: Cambridge, UK, 2013. [CrossRef]
36. Piskorowski, J. A new concept of filters for biomedical data processing needs. *Biocybern. Biomed. Eng.* **2011**, *31*, 27–37. [CrossRef]
37. D'agostino, R.B.; Belanger, A.; D'agostino, R.B., Jr. A Suggestion for Using Powerful and Informative Tests of Normality. *Am. Stat.* **1990**, *44*, 316–321. [CrossRef]
38. Xiaodong, Z.; Haojie, L. Study on measurement and processing technology of electromyography. In Proceedings of the 2007 8th International Conference on Electronic Measurement and Instruments, Xi'an, China, 16–18 August 2007; IEEE: Piscataway, NJ, USA, 2007.
39. Zhou, R.; Luo, Q.; Feng, X.; Li, C. Design of a wireless multi-channel surface EMG signal acquisition system. In Proceedings of the 2017 3rd IEEE International Conference on Computer and Communications (ICCC), Chengdu, China, 13–16 December 2017; IEEE: Piscataway, NJ, USA, 2017.
40. Yoo, J.; Yan, L.; El-Damak, D.; Altaf, M.A.B.; Shoeb, A.H.; Chandrakasan, A.P. An 8-channel scalable EEG acquisition SoC with patient-specific seizure classification and recording processor. *IEEE J. Solid-State Circuits* **2013**, *48*, 214–228. [CrossRef]
41. Moradi, M.; Dousti, M.; Torkzadeh, P. Designing a low-power LNA and filter for portable EEG acquisition applications. *IEEE Access* **2021**, *9*, 71968–71978. [CrossRef]
42. Lu, T.C.; Liu, P.; Gao, X.; Lu, Q.Y. A Portable ECG Monitor with Low Power Consumption and Small Size Based on AD8232 Chip. *Appl. Mech. Mater.* **2014**, *513*, 2884–2887. [CrossRef]

43. Vishwakarma, P.K.; Singh, R. A—Review on IoT-Assisted ECG Monitoring Framework for Health Care Applications. In Proceedings of the 2021 Fourth International Conference on Computational Intelligence and Communication Technologies (CCICT), Sonepat, India, 3 July 2021; pp. 203–207. [CrossRef]
44. Umar, U.; Nayab, S.; Irfan, R.; Khan, M.A.; Umer, A. E-Cardiac Care: A Comprehensive Systematic Literature Review. *Sensors* **2022**, *22*, 8073. [CrossRef]
45. Agung, M.A.; Basari. 3-lead acquisition using single channel ECG device developed on AD8232 analog front end for wireless ECG application. *AIP Conf. Proc.* **2017**, *1817*, 040015. [CrossRef]
46. Machado, R.C. A Wearable System for Heart Failure Monitoring. Ph.D. Thesis, Universidade de Coimbra, Coimbra, Portugal, 2020.
47. PLUX—Wireless Biosignals, S.A. Electromyography (EMG) Sensor Data Sheet. 2020. Rev.B. Available online: https://support.pluxbiosignals.com/wp-content/uploads/2021/11/emg-sensor-datasheet-assembled-1.pdf (accessed on 8 August 2022).
48. PLUX—Wireless Biosignals, S.A. Electromyography (EMG) Sensor Data Sheet. 2016. Rev.A. Available online: https://support.pluxbiosignals.com/wp-content/uploads/2021/11/revolution-emg-sensor-datasheet-1.pdf (accessed on 8 August 2022).
49. Batista, D.; Plácido da Silva, H.; Fred, A.; Moreira, C.; Reis, M.; Ferreira, H.A. Benchmarking of the BITalino biomedical toolkit against an established gold standard. *Healthc. Technol. Lett.* **2019**, *6*, 32–36. [CrossRef] [PubMed]
50. Zompanti, A.; Sabatini, A.; Grasso, S.; Pennazza, G.; Ferri, G.; Barile, G.; Chello, M.; Lusini, M.; Santonico, M. Development and Test of a Portable ECG Device with Dry Capacitive Electrodes and Driven Right Leg Circuit. *Sensors* **2021**, *21*, 2777. [CrossRef]
51. Bravo-Zanoguera, M.; Cuevas-González, D.; Reyna, M.A.; García-Vázquez, J.P.; Avitia, R.L. Fabricating a Portable ECG Device Using AD823X Analog Front-End Microchips and Open-Source Development Validation. *Sensors* **2020**, *20*, 5962. [CrossRef] [PubMed]
52. Jung, J.; Lee, D.W.; Son, Y.; Kim, B.; Gu, J.; Shin, H.C. Volitional EMG Controlled Wearable FES System for Lower Limb Rehabilitation. In Proceedings of the 2021 43rd Annual International Conference of the IEEE Engineering in Medicine & Biology Society (EMBC), Mexico, Virtual Conference, 1–5 November 2021; IEEE: Piscataway, NJ, USA, 2021; pp. 7099–7102.
53. Diego, J.R.; Martinez, D.W.C.; Robles, G.S.; Dizon, J.R.C. Development of smartphone-controlled hand and arm exoskeleton for persons with disability. *Open Eng.* **2020**, *11*, 161–170. [CrossRef]
54. Chapman, J.; Dwivedi, A.; Liarokapis, M. A Wearable, Open-Source, Lightweight Forcemyography Armband: On Intuitive, Robust Muscle-Machine Interfaces. In Proceedings of the 2021 IEEE/RSJ International Conference on Intelligent Robots and Systems (IROS), Prague, Czech Republic, 27 September–1 October 2021; pp. 4138–4143. [CrossRef]
55. Krueger, E.; Popović-Maneski, L.; Neto, G.N.N.; Mendonça Scheeren, E.; Fiusa, J.M.; Nohama, P. Neuromuscular fatigue detection by mechanomyography in people with complete spinal cord injury. *Res. Biomed. Eng.* **2020**, *36*, 203–212. [CrossRef]

Disclaimer/Publisher's Note: The statements, opinions and data contained in all publications are solely those of the individual author(s) and contributor(s) and not of MDPI and/or the editor(s). MDPI and/or the editor(s) disclaim responsibility for any injury to people or property resulting from any ideas, methods, instructions or products referred to in the content.